

Supplemental Materials

Supplementary Table. 1: Human pancreas donors obtained from Network for Pancreatic Organ Donors with Diabetes (nPOD).

Supplementary Fig. 1: Characterization of SDHB^{βKO} mice.

Supplementary Fig. 2: Immunofluorescent staining in ND Human Pancreas.

Supplementary Fig. 3: Islet Insulin Content in Control and SDHB^{βKO} islets.

Supplementary Fig. 4: Metabolomic analysis in Control and SDHB^{βKO} islets.

Supplementary Fig. 5: RNA Sequencing in Control and SDHB^{βKO} islets.

Supplementary Fig. 6: Pathway Changes of SDHB^{βKO} Islets based on Metabolomics and Transcriptomics Analyses.

Supplementary Fig. 7: Rapamycin reduces succinate levels, $\Delta\Psi_m$ and lipid content in 3-NPA- and DMS-treated R7T1 β -cells.

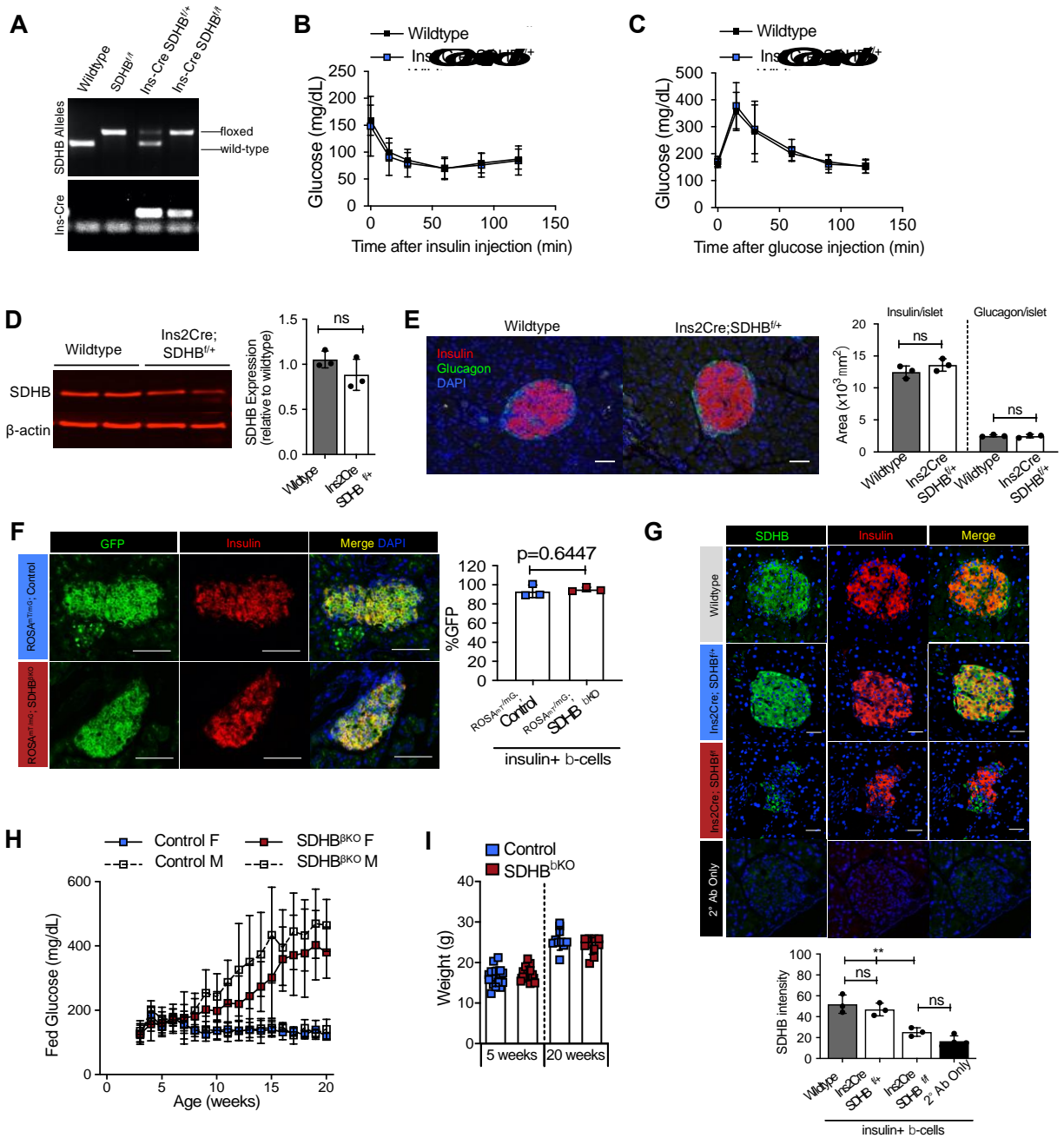
Supplementary Fig. 8: Rapamycin effect on GSIS *in vivo*.

Supplementary Table 1

| CaseID | Age (yrs) | Sex | BMI | Race | Donor Type |
|---------------|------------------|------------|------------|-----------------|-------------------|
| 6020 | 60 | M | 29.8 | Caucasian | ND |
| 6102 | 45 | F | 35.1 | Caucasian | ND |
| 6015 | 39 | F | 32.2 | Caucasian | ND |
| 6288 | 55 | M | 37.7 | Caucasian | ND |
| 6009 | 45 | M | 30.6 | Caucasian | ND |
| 6251 | 33 | F | 29.5 | Caucasian | ND |
| 6254 | 38 | M | 30.5 | Caucasian | ND |
| 6234 | 20 | F | 25.6 | Caucasian | ND |
| 6108 | 58 | M | 30.4 | Asian | T2D |
| 6127 | 45 | F | 30.4 | Caucasian | T2D |
| 6139 | 37 | F | 45.4 | Hispanic/Latino | T2D |
| 6259 | 57 | M | 32.3 | Caucasian | T2D |
| 6275 | 48 | M | 41.0 | Hispanic/Latino | T2D |
| 6249 | 45 | F | 32.3 | Asian | T2D |
| 6252 | 20 | M | 37.8 | Caucasian | T2D |

Supplementary Table. 1: Human pancreas donors obtained from Network for Pancreatic Organ Donors with Diabetes (nPOD). Organ donor information: Age (years), Sex, Body Mass Index (BMI), No Diabetes (ND) and Type 2 Diabetes (T2D).

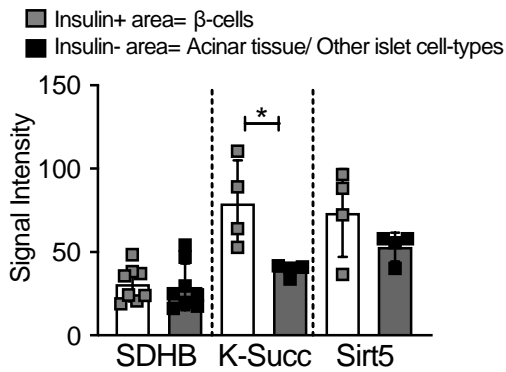
Supplementary Figure 1



Supplementary Fig. 1: Characterization of SDHB^{BKO} mice. **A:** Agarose gel of *sdhb* DNA isolated from tail snips for verification of mouse genotype. **B,C:** Glucose levels following (B) intraperitoneal insulin (0.75 IU/kg) and (C) intraperitoneal glucose (2 mg/kg) administration in 5-week-old wild-type and Ins2Cre; SDHB^{f/+} (heterozygous Control) mice (n=9/group). **D:** Representative immunoblot of SDHB protein in islet lysates from 5-week-old wild-type and

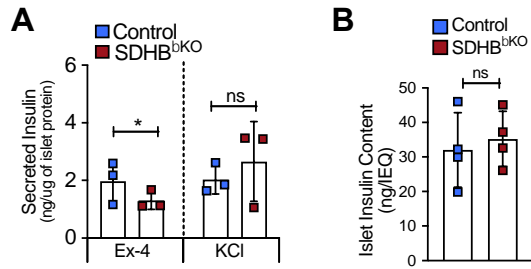
Ins2Cre; SDHB^{f/+} (n=3 mice/group). Quantification of SDHB expression normalized to β -actin loading control. **E:** Representative immunofluorescent images pancreatic sections from 5-week-old wild-type and Ins2Cre; SDHB^{f/+} mice stained with insulin (red) and glucagon (green). Nuclei were counterstained with DAPI. Scale Bar, 50 μ M. Quantification of insulin and glucagon positive areas per islet in pancreatic sections are shown in the adjacent graph (n=3 mice/group). **F:** Percentage of Cre-expressing β -cells. Representative immunofluorescent images of GFP (green) and insulin (red) staining in pancreatic sections from 5-week-old fluorescent Cre-reporter mice- ROSA^{mTmG} Control and ROSA^{mTmG} SDHB ^{β KO}. Quantification of mean % GFP-positive cells within insulin+ β -cells \pm SD are shown in adjacent graphs (n= five images/mice from 3 mice/group). **G:** Representative immunofluorescent images of SDHB in pancreatic sections from 5-week-old wild-type, Ins2Cre; SDHB^{f/+} (heterozygous Control) and Ins2Cre; SDHB^{f/f} (SDHB ^{β KO}) mice. Quantification of mean staining intensity \pm SD within insulin+ β -cells are shown in adjacent graph (n= five images/mice from 3 mice/group). Secondary antibody only (2^o Ab) serves as no primary antibody background control. **H:** Sex-specific representation of mean random (free-fed) blood glucose levels \pm SD in female verse male Control and SDHB ^{β KO} mice (3-20 weeks), n=20/group. **I:** Mixed gender animal weights (g) of control and SDHB ^{β KO} mice at 5 and 20 weeks, n=10-16 mice/group.

Supplementary Figure 2



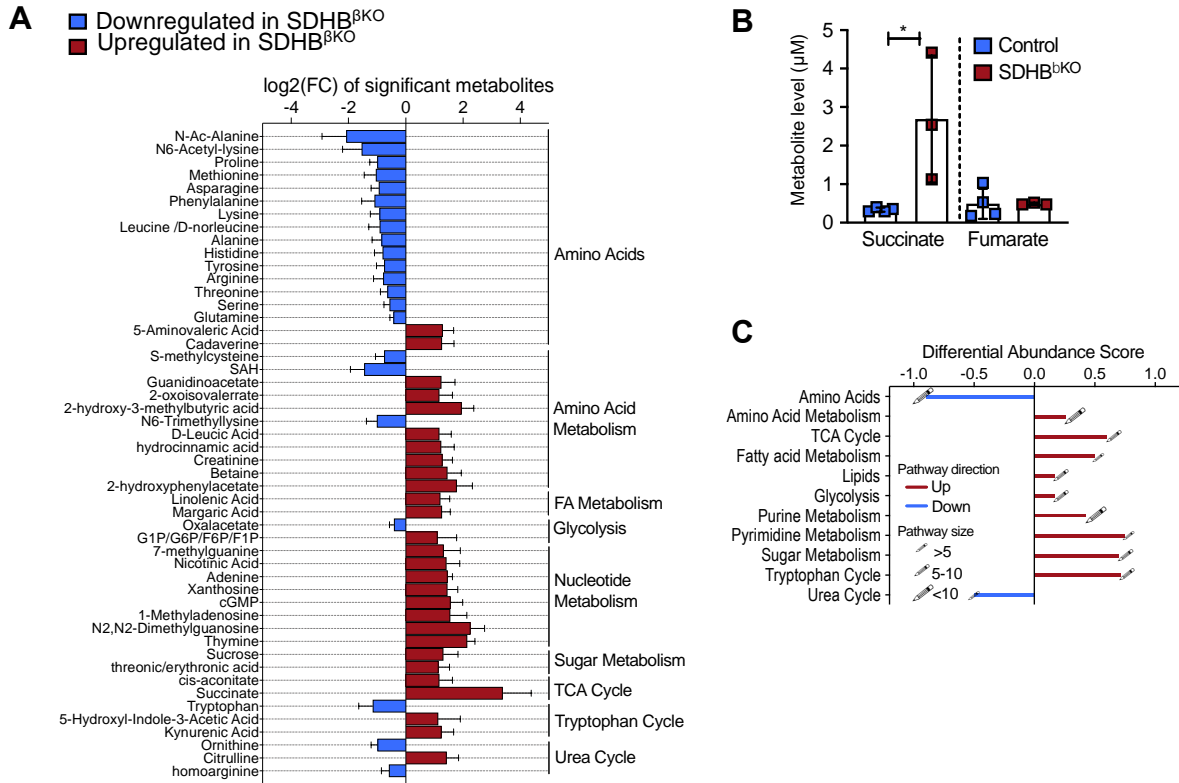
Supplementary Fig. 2: Immunofluorescent staining in ND Human Pancreas. Quantification of mean SDHB, K-Succ and Sirt5 staining intensity in either the insulin-positive β -cells or insulin-negative areas (acinar tissue and other islet-cell types) of pancreas sections from human donor (n=4-6 islets/donor from n=4-8 donors/group). Data represented as mean \pm SD and were analyzed by unpaired t-test. *, $p < 0.05$.

Supplementary Figure 3



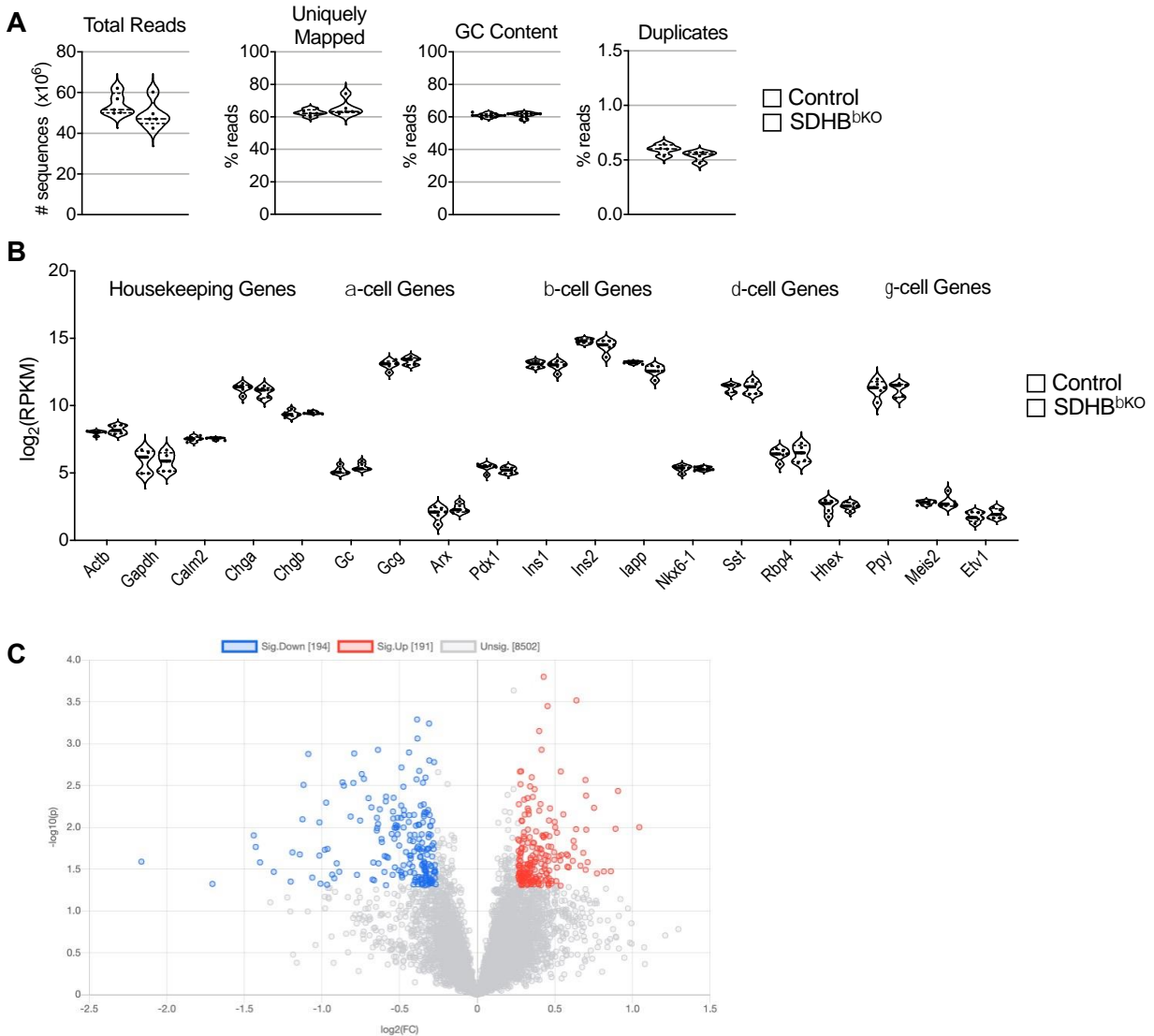
Supplementary Fig. 3: Islet Insulin Content. **A:** Static insulin secretion response to high glucose [16.7 mM] + 20 nM exendin-4 (Ex-4) and basal glucose [5.6 mM] + 20 mM potassium chloride (KCl) in isolated islets from 5-week-old Control and SDHB^{βKO}, n=3 mice/group. **B:** Insulin content of 5-week-old Control and SDHB^{βKO} islets used for islet perfusion assay, n=4/group.

Supplementary Figure 4



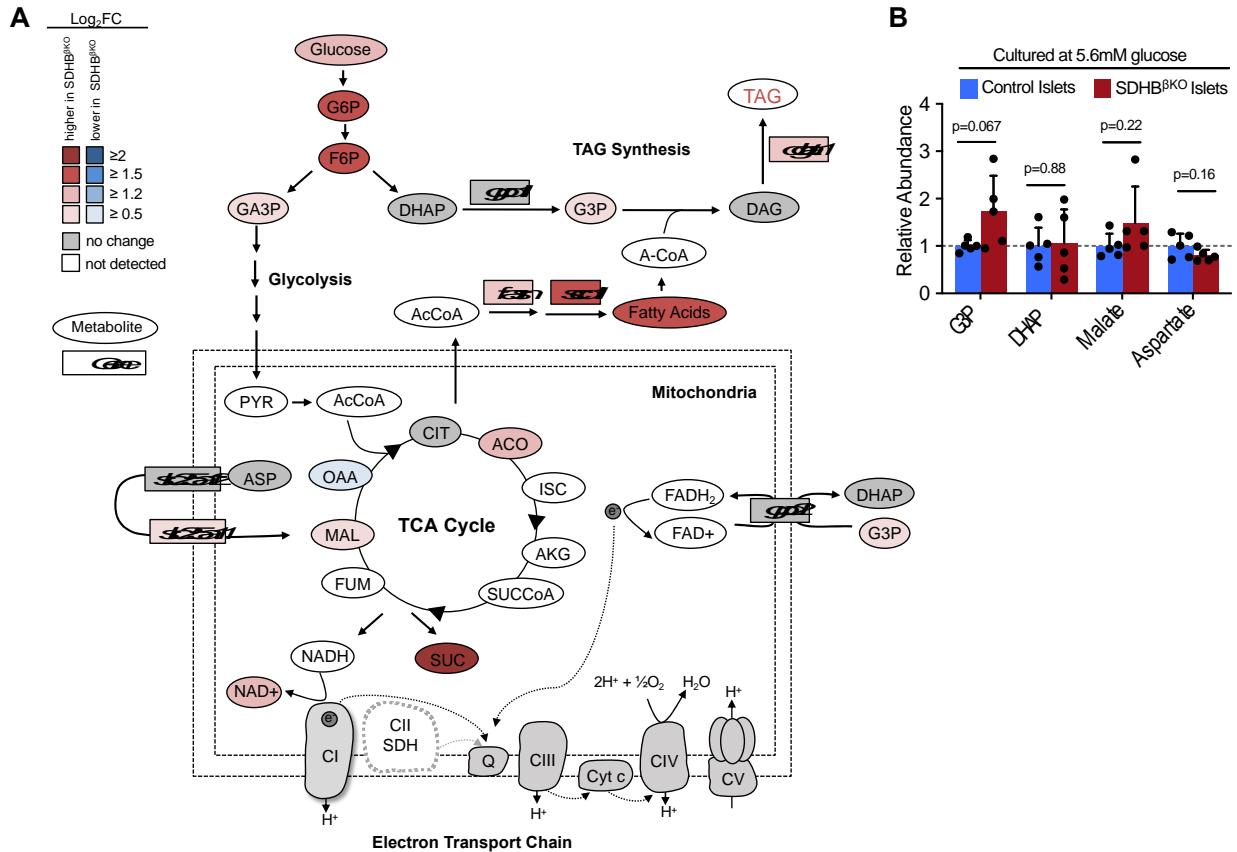
Supplementary Fig. 4: Metabolomic analysis. From 148 identified metabolites, we observed significant changes in 50 metabolites ($p < 0.05$), where 28 were increased ($\text{Log}_2\text{FC} \geq 1$) and 22 were decreased ($\text{Log}_2\text{FC} \leq -1$) in SDHB^{BKO} islets. **A:** Fold-change \pm SEM of significantly (p -value < 0.05) downregulated and upregulated metabolites identified in SDHB^{BKO} islets, compared to Ins2-Cre SDHB^{fl/wt} (Control) islets, $n=5/\text{group}$. Metabolites are categorized into specific metabolic pathways. **B:** Succinate and fumarate levels (μM) measured by LC-MS/MS in isolated islets from 5-week-old Ins2-Cre SDHB^{fl/wt} (Control; $n=4$) and SDHB^{BKO} mice ($n=3$). **C:** Data represented as mean \pm SD and were analyzed by unpaired t-test. *, $p < 0.05$. Metabolic pathway-based analysis with differential abundance scores. The differential abundance score captures the average, gross changes for all metabolites in a pathway. A score of 1 indicates all measured metabolites in the pathway increase, and -1 indicates all measured metabolites in a pathway decrease.

Supplementary Figure 5



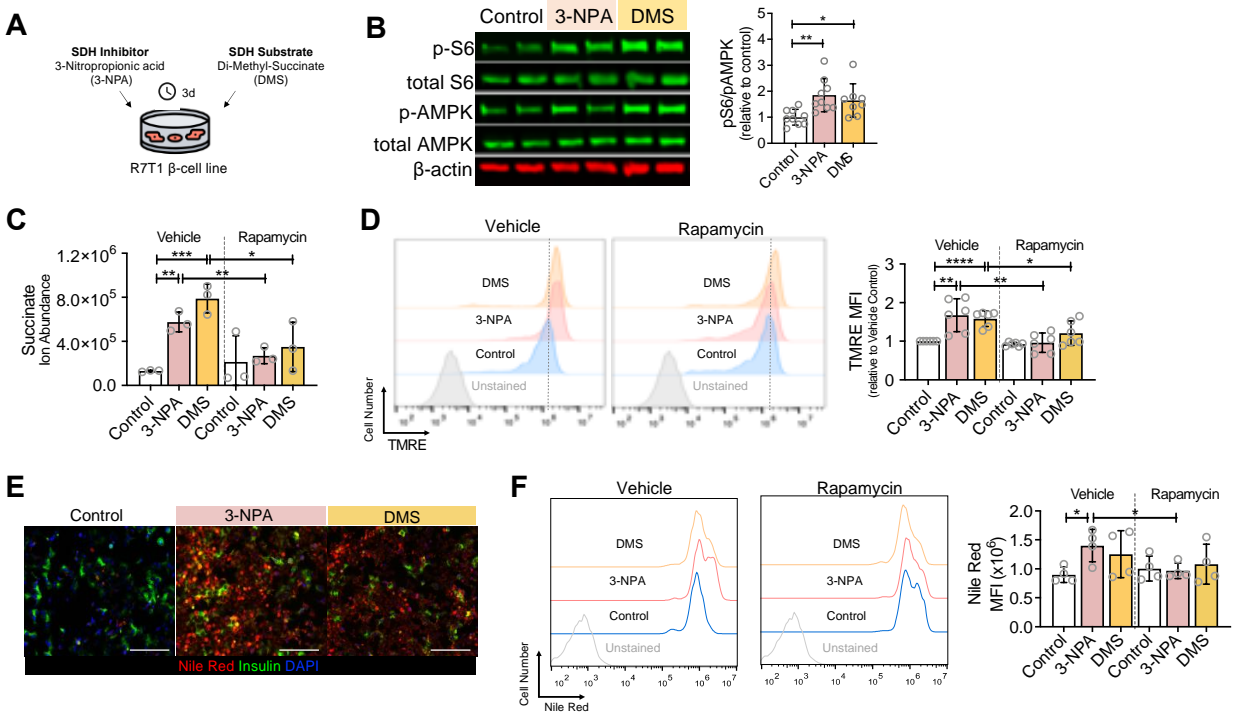
Supplementary Fig. 5: RNA Sequencing in Control and SDHB^{βKO} islets. From 30,447 identified genes, 385 were differentially expressed in SDHB^{βKO} islets compared to Ins2Cre; SDHB^{f/+} (Control) islets ($p < 0.05$). Of these, 194 genes were up-regulated and 191 genes were down-regulated. **A:** RNA-seq data quality control metrics: total reads (# of sequences reads) and uniquely mapped, duplicates and GC content (as % of total reads). **B:** Key expression genes (*Camunas-Soler et al, Cell Metab, 2020*) for each islet cell-type identified in transcriptomic analysis: α -, β -, δ -, and γ -cells. **C:** Volcano plot of differentially expressed genes in SDHB^{βKO} compared to Control. Red: up-regulated genes ($\text{LogFC} \geq 1.2$); Blue: down-regulated genes ($\text{LogFC} \geq -1.2$).

Supplementary Figure 6



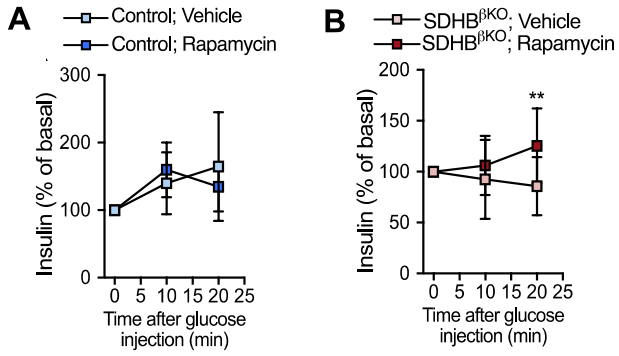
Supplementary Fig. 6: Pathway Changes of SDHB^{BKO} Islets based on Metabolomics and Transcriptomics Analyses. **A:** Schematic representation of pathway changes. Color corresponds to the Log₂ fold changes between in SDHB^{BKO} and Ins2Cre; SDHB^{f/+} (Control) islets. Red, increase; blue, decrease; gray, no change; white, not detected/measured. Metabolites are labelled as color-coded ovals: A-Coa, acyl-CoA; AcCoA, acetyl-CoA; ACO, cis-aconitate; AKG, alpha-ketoglutarate; ASP, aspartate; CIT, citrate; DAG, diacylglyceride; DHAP, dihydroxyacetone phosphate; F6P, fructose 6-phosphate; FUM, fumarate; G6P, glucose 6-phosphate; G3P, glyceraldehyde 3-phosphate; GA3P, glyceraldehyde 3-phosphate; ISC, isocitrate; MAL, malate; OAA, oxaloacetate; PYR, pyruvate; SUCCoA, succinyl-CoA; SUC, succinate. Transcript genes are labelled as color-coded rectangles: *dgat1*, diacylglycerol o-acyltransferase 1; *fasn*, fatty acid synthase; *gpd1/2*, glycerol-3-phosphate dehydrogenase 1/2; *slc25a11*, 2-oxoglutarate/malate carrier; *slc25a12*, aspartate/glutamate carrier. **B:** Basal metabolite levels associated with G3P and malate-aspartate shuttle in isolated islets from 5-week-old Ins2-Cre SDHB^{f/wt} (Control) and SDHB^{BKO} mice (n=5/group). Data represented as mean ± SD and were analyzed by unpaired t-test.

Supplementary Figure 7



Supplementary Fig. 7: Rapamycin reduces succinate levels, $\Delta\Psi_m$ and lipid content in 3-NPA- and DMS-treated R7T1 β -cells. **A:** Graphical representation of treatment experiments in R7T1 β -cell culture. R7T1 β -cells are treated with 3-Nitropropionic acid (3-NPA) and cell-permeable dimethyl-succinate (DMS) for 3 days. **B:** Representative immunoblot of cell lysates from control, 3-NPA and DMS-treated R7T1 β -cells. β -actin serves as the loading control. Quantification of immunoblot as a ratio of p-S6 over phospho-AMPK α shown in adjacent graphs, n=8-9/group from three independent experiments. **C:** Cellular succinate levels in 3-NPA and DMS-treated R7T1 β -cells with a 24h vehicle or rapamycin [50 nM] treatment, n=3/group. **D:** Representative FACS analyses of mitochondrial membrane potential (TMRE) in 3-NPA and DMS-treated R7T1 β -cells following a vehicle or rapamycin treatment. Median Fluorescence Intensity (MFI) of TMRE relative to vehicle control shown in adjacent graph, n=6/group from three independent experiments. **E:** Representative immunofluorescent images of control, 3-NPA and DMS-treated R7T1 β -cells stained with Nile Red (red) and insulin (green). Nuclei were counterstained with DAPI. **F:** Representative FACS analyses of Nile Red in control, 3-NPA and DMS-treated R7T1 β -cells after a 24h treatment with vehicle or rapamycin. Median Fluorescence Intensity (MFI) of Nile Red is shown in adjacent graph, n=4/group from two independent experiments.

Supplementary Figure 8



Supplementary Fig. 8: Rapamycin effect on GSIS *in vivo*. Serum insulin levels following intraperitoneal glucose (10 mg/kg) injection in (A) control and (B) SDHB^{βKO} mice, n=12-14/group.